Photoemission Spectroscopy of Magnetic and Nonmagnetic Impurities on the Surface of the Bi_2Se_3 Topological Insulator

T. Valla,[1,*] Z.-H. Pan,[1] D. Gardner,[2] Y. S. Lee,[2] and S. Chu[3]

[1]*Condensed Matter Physics and Materials Science Department, Brookhaven National Lab, Upton, New York 11973, USA*
[2]*Department of Physics, Massachusetts Institute of Technology, Cambridge, Massachusetts 02139, USA*
[3]*Center for Materials Science and Engineering, Massachusetts Institute of Technology, Cambridge, Massachusetts 02139, USA*

(Received 6 April 2011; published 12 March 2012)

Dirac-like surface states on surfaces of topological insulators have a chiral spin structure that suppresses backscattering and protects the coherence of these states in the presence of nonmagnetic scatterers. In contrast, magnetic scatterers should open the backscattering channel via the spin-flip processes and degrade the state's coherence. We present angle-resolved photoemission spectroscopy studies of the electronic structure and the scattering rates upon the adsorption of various magnetic and nonmagnetic impurities on the surface of Bi_2Se_3, a model topological insulator. We reveal a remarkable insensitivity of the topological surface state to both nonmagnetic and magnetic impurities in the low impurity concentration regime. Scattering channels open up with the emergence of hexagonal warping in the high-doping regime, irrespective of the impurity's magnetic moment.

DOI: 10.1103/PhysRevLett.108.117601 PACS numbers: 79.60.−i, 63.20.−e, 71.18.+y, 74.10.+v

Topological insulators (TIs) belong to a new class of insulators in which the bulk gap is inverted due to the strong spin-orbit coupling. On the boundaries or interfaces of these materials with ordinary (''trivial'') insulators, gapless states inevitably occur, topologically protected by the time-reversal symmetry [1–3]. Three-dimensional topological insulators have surface states with an odd number of massless Dirac cones in which the spin of an electron is locked perpendicular to its momentum in a chiral spin-structure, where electrons with opposite momenta have opposite spins [4–10]. A direct consequence of this spin-momentum locking is that a backscattering, which would require a spin-flip process, is not allowed if a time-reversal-invariant perturbation, such as nonmagnetic disorder, is present [4]. This makes topological insulators potentially very promising materials that could serve as a platform for spintronics and for quantum computing applications, where spin-coherence is crucial. In contrast, a time-reversal symmetry breaking perturbation, such as the introduction of magnetic impurities on the surface, is expected to open a backscattering channel and induce a gap at the Dirac point of the topological surface state (TSS) [11–17].

Even though it might be expected that these fundamental predictions would be checked very quickly, the experiments that would directly probe the sensitivity of the TSS and differentiate between the two types of disorder are still lacking. Scanning tunneling microscopy experiments have shown that backscattering is indeed strongly suppressed or completely absent, despite the strong atomic scale disorder [18–20]. In angle-resolved photoemission spectroscopy (ARPES), there has been very little quantitative work on the scattering rates. One study [21] has indicated that the major decay channel for the TSS is scattering into the bulk states, either elastically, on defects, or inelastically, via the electron-electron interaction. More recent studies have also shown that the adsorption of various nonmagnetic atomic or molecular species on the surface of a topological insulator induces electronic doping and partial filling of additional spin-orbit split states [22,23]. It has been also suggested that magnetic impurities, both in the bulk and on the surface, open a small gap at the Dirac point [16,17]. However, the most fundamental question—how the magnetic moment of an impurity affects the scattering—has remained unanswered. Even for nonmagnetic perturbations, it would be highly desirable to know how the TSS behaves as the concentration of impurities increases and how it is affected by the presence of other states that become partially occupied by electron doping. Would the presence of such states, that come in spin-orbit split pairs, therefore allowing interband scattering, both with and without spin-flip, degrade the TSS's coherence? Or, would the intraband scattering dominate? We note that none of these questions have been addressed in experiments and that there has been no systematic studies of the scattering rates on any kind of impurities.

Here, we present quantitative experimental studies of scattering rates on the surface of Bi_2Se_3, a model TI. We directly compare the effects of non- magnetic and magnetic impurities on the TSS and, quite unexpectedly, we find that there is essentially no difference between these two types of scatterers. Both the scattering and the impurity induced development of the surface electronic structure seem remarkably insensitive to the type of disorder. Instead, we find that the scattering rates are sensitive to the Fermi surface shape, which can be tuned by the doping, irrespective of the impurity's magnetic moment. We also

find no evidence for an opening of a gap at the Dirac point of the TSS.

The single-crystal samples were synthesized by mixing stoichiometric amounts of bismuth and selenium with trace amounts of arsenic in evacuated quartz tubes [24]. The ARPES experiments were carried out at the U13UB beamline of the National Synchrotron Light Source with the photons in the range between 15.5 and 22 eV. The electron analyzer was a Scienta SES-2002 with the combined energy resolution around 8 meV and the angular resolution of $\sim 0.15°$. Samples were cleaved *in situ* in the UHV chamber with the base pressure of 3×10^{-9} Pa. Ni was deposited using an *e*-beam evaporator, Cu and Gd were evaporated from a resistively heated tungsten basket, while alkali-metal atoms were deposited from commercial (SAES) getter sources with the samples kept at ~ 15 K during the deposition and ARPES measurements.

Figure 1 shows the development of the surface electronic structure upon deposition of rubidium on the Bi_2Se_3 surface. The rapidly dispersing conical band in the pristine sample represents the TSS with the Dirac point around 0.32 eV below the Fermi level. At a binding energy higher than 0.4 eV, the TSS overlaps with the bulk valence band and near the Fermi level, the bulk conducting band is visible inside the surface state cone, indicating the electron doping of Bi_2Se_3 by Se vacancies. The TSS has an almost perfectly circular Fermi surface. Upon Rb deposition, TSS is further doped with electrons, which is evident from the down-shift of the Dirac point and the growing Fermi surface that acquires a pronounced hexagonal warping. However, this is not the only effect of doping: New states are also being formed and progressively filled with electrons donated by adsorbed Rb. In panels (c) and (d) we show the stage of Rb deposition at which the maximal charge transfer into the surface electronic structure of Bi_2Se_3 is reached. At this stage, in addition to the original TSS, two pairs of new states are visible at lower binding energies. Each pair consists of two spin-orbit split states, displaced in momentum in a Rashba-type manner, intersecting at new Dirac points at the zone center. These states also have surface character as they do not disperse with k_z. At the highest doping levels, the outermost state becomes almost degenerate with the TSS, forming the Fermi surface nearly equal in shape and size. Its inner counterpart is significantly smaller, retaining the perfectly circular Fermi surface, even at the highest doping. We also observe new valence states below the Dirac point of the TSS. Although their dispersion near the zone center resembles the dispersion of the bulk valence band, the lack of k_z dispersion indicates their surface character.

Figure 1(e) summarizes the changes in some of the measured quantities with Rb doping. The surface doping level was determined by measuring the Fermi surface area of the TSS and of the lower Rashba-split doublet: A_T (TSS), A_O (outer Rashba state), and A_I (inner Rashba state). The upper Rashba doublet was not taken into account. The total charge (per surface unit cell) is then $q = (A_T + A_O + A_I)/A_{\mathrm{BZ}}$, where $A_{\mathrm{BZ}} = 2.662$ Å^{-1} represents the Brillouin zone area. At maximal doping, nearly $0.105e^-$ per surface unit cell is transferred from Rb into the three states shown here. If the second pair of states [better resolved in Fig. 2(c)] is counted, then the total charge transfer is $\sim 0.14e^-$. The surface charge density $n = q/A_{\mathrm{UC}}$, where $A_{\mathrm{UC}} = 44.487$ Å^2 is the area of the unit cell in real space, could be tuned from $\sim 1 \times 10^{12}$ cm^{-2} (clean sample) to $\sim 5 \times 10^{13}$ cm^{-2} (maximal doping). As

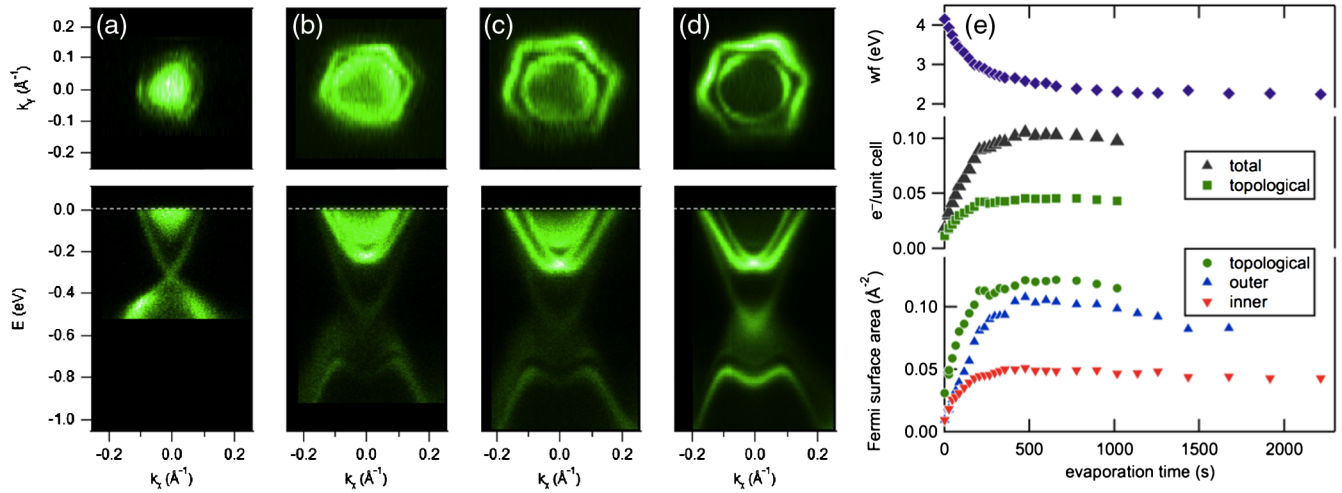

FIG. 1 (color online). Surface doping of Bi_2Se_3. (a) to (d) ARPES spectra from Bi_2Se_3 at various stages of Rb deposition, showing the Fermi surface (upper panels) and the (E, k) dispersion of photoemission intensity along the momentum line slightly off the ΓM line in the surface Brillouin zone (lower panels). (a) pristine surface, (b) intermediate doping, and (c) maximal doping, taken at $h\nu = 21.3$ eV and at $h\nu = 18.7$ eV (d). (e) Fermi surface area of the TSS and of the lower Rashba doublet (bottom), charge doped into these states (middle) and the work function (top) as functions of Rb deposition time.

a Rb atom can donate at most one electron, the measured charge transfer implies that the average Rb-Rb distance could be shorter than 3 unit cells. Scattering on Rb would then lead to the very short mean free path for surface electrons ($\sim$ 3 surface unit cells). However, Fig. 1 suggests that all the states are still very coherent, with the mean free paths $\ell = 1/\Delta k$ in the range of 100 Å, where Δk is the momentum spread of the Fermi surface, measured from the momentum distribution curves [25]. Insensitivity to impurity scattering might be expected for the TSS, but only in the absence of other states that could open the interband scattering channels. Thus, the retained coherence of all the detected states is somewhat surprising.

In Fig. 2, we compare the effects of different adsorbates on the surface electronic structure of Bi_2Se_3—in particular we compare the nonmagnetic impurities, Rb and Cs, with Gd, whose atoms have large magnetic moments, $\sim 8\mu_B$. We have also studied adsorbed Ni and Cu (not shown).

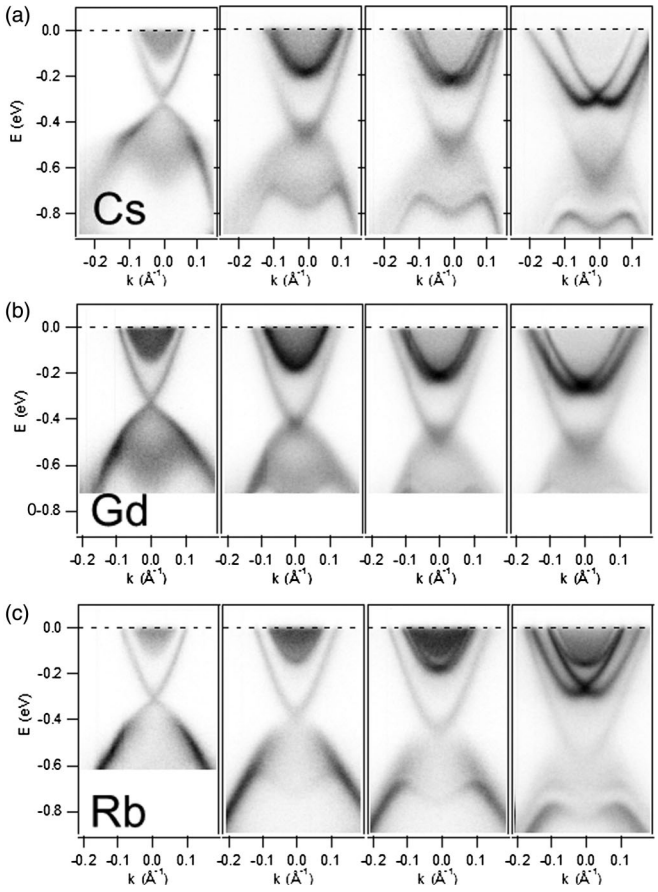

FIG. 2. Development of the surface electronic structure with Cesium (a), Gadolinium (b), and Rubidium (c) adsorption at the surface of Bi_2Se_3. The spectra were recorded along the ΓM line in the surface Brillouin zone and at $h\nu = 18.7$ eV for Cs and Gd, and along the ΓK line and at $h\nu = 21.3$ eV for Rb. The leftmost panels correspond to the pristine surface, while the rightmost panels show the electronic structure near the maximal doping achieved with each dopand.

Surprisingly, there is no visible difference in the spectra for different adsorbates, if taken at the same photon energy. In the recent study where iron was deposited on Bi_2Se_3, the electronic structure also looks very similar [17]. Relative intensities of the states that form the Fermi surface depend on photon energy, reflecting the variation of ARPES matrix elements. Thus, the higher pair of Rashba-split states, hardly visible in Cs- and Gd-covered surfaces, is clearly resolved in the Rb doped system, which is measured at different photon energy. However, none of these states disperse with k_z, reflecting their surface character. We also note that the maximal doping level achievable with different adsorbates increases from Ni to Gd to Cu to Rb to Cs.

The most important observation from the spectra in Fig. 2 is that, contrary to the expectations, the magnetic state of the adsorbate does not seem to play a significant role in the scattering. At similar stages of doping with different adsorbates, the TSS seems similarly coherent. The same is true for the Rashba-split states. Further, it appears that all the adsorbates have a similar effect on the spectral region around the Dirac point of TSS, with no clear gap formation.

In Fig. 3 we show the imaginary part of the quasiparticle self-energy, $|\mathrm{Im}\Sigma(\omega)| = \Gamma(\omega)/2$, where $\Gamma(\omega)$ represents the scattering rate, as a function of binding energy for TSS for several different concentrations of Rb and Gd atoms on the surface of Bi_2Se_3. Scattering rates are determined from $\Gamma(\omega) = 2|\mathrm{Im}\Sigma(\omega)| = \Delta k(\omega) v_0(\omega)$, where $\Delta k(\omega)$ is the measured full width at half maximum of the Lorentzian-fitted peak in the momentum distribution curve, and $v_0(\omega)$ is the group velocity of the state at energy ω. The TSS remains very coherent until the concentration of adsorbed atoms reaches the level at which the Fermi surface

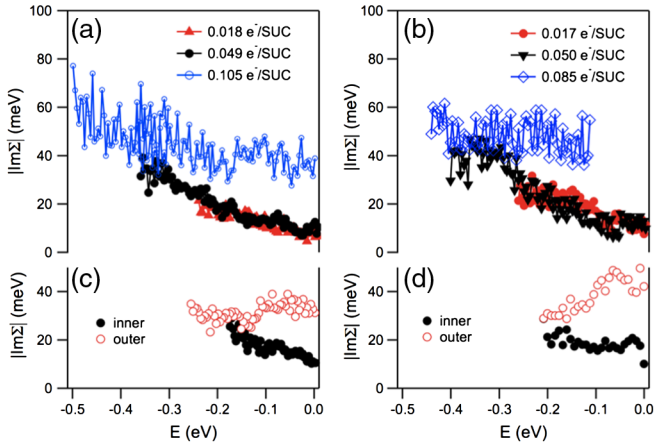

FIG. 3 (color online). $\mathrm{Im}\Sigma(\omega)$ of the topological surface state upon adsorption of Rubidium (a) and Gadolinium (b) for several different doping levels, as indicated. (c) and (d) show $\mathrm{Im}\Sigma(\omega)$ of the lower Rashba-split doublet for Rb and Gd doped surfaces, respectively, near the maximum doping.

becomes heavily hexagonally warped, regardless of whether the adsorbates are magnetic or nonmagnetic. For similar doping levels, the scattering rates are essentially the same for Rb- and Gd-covered surfaces. Pristine surfaces, and surfaces with relatively low concentration of impurities, show very low ImΣ at the Fermi level, indicating long coherence lengths of TSS, $\ell > 150$ Å. Even at the doping levels $\sim 0.05e^-$ per surface unit cell, where the average distance between the impurities is shorter than ~ 5 unit cells, the TSS remains unaffected. ImΣ slowly increases with energy as $\propto \omega^2$, indicating that the inelastic electron-electron scattering has a Fermi-liquid–like form. For high impurity concentrations, $\sim 0.1e^-$ per surface unit cell, ImΣ reaches the value of ~ 40 meV at the Fermi level, corresponding to the mean free path of ~ 70 Å, and is nearly energy independent. Because of the partial overlap with the significantly more intense outer Rashba state, we could not reliably determine the width of the TSS at low energies. We also show the ImΣ for the two states that form the lower Rashba-split doublet. There is a significant difference between the states forming the doublet: the outer state is significantly broader than the inner one and is similar in width to the TSS at this concentration level. This is again true for both magnetic and nonmagnetic impurities.

In Fig. 4 we illustrate the effects of Cs and Gd deposition on the spectral region near the Dirac point of TSS. We show the spectral intensity at the point slightly displaced from the $k_x = 0$ (middle panels) and exactly at the $k_x = 0$ point (right panels), as a function of Cs and Gd deposition time. Contrary to the expectations, both metals have similar effects: with the deposition of these metals, it seems as if the lower and the upper parts of the Dirac cone penetrate each other. Thus, at small but finite k_x, the two branches merge and possibly intersect after ~ 6 min of evaporation. If the gap opens at the Dirac point, as might be expected for magnetic impurities, the upper and the lower branch of the TSS cone should remain separated. The separation should also occur at $k_x = 0$, once the gap opens. Our results suggest that neither of the adsorbates opens a clear gap at the Dirac point of the TSS. We also see no evidence of a gap at the second Dirac point, where the states forming the lower Rashba-split doublet intersect (Fig. 2). This suggests that the Kramer's points, i.e., the points where the spins are degenerated in the unperturbed system, are more robust to magnetic perturbations than expected. One possible reason for this insensitivity could be a strongly localized magnetic moment (f orbitals) in adsorbed Gd, resulting in a very small scattering cross section. However, similar results for adsorbed nickel and iron [17] with the more delocalized moments, would argue against this explanation.

Our experiments show that the quasiparticle scattering on the surface of a TI is not affected by magnetic moments of impurity atoms. This might imply that the scattering rates are dominated by the small momentum transfer events and not by backscattering. Then, the existence of multiple Fermi surfaces, allowing both the intraband and interband scattering, and the observation that the inner Rashba-split Fermi surface is always sharper than its outer counterpart and the TSS, might suggest that the former one has the opposite spin helicity than the latter two. However, recent calculations [17] suggest that the spin helicities of these three states alternate (left-right-left). If this is the case, our results would imply that the interband scattering is strongly suppressed. Indeed, we do not see any anomalies in the scattering rates at the thresholds for the interband channels. Therefore, we could conclude that the observed broadening with adsorption of impurities reflects the increase in intraband scattering as the size and the warping of the Fermi surface grows with doping [9,11,13,26,27]. We note that these effects will likely play the determining role in a performance of any electronic device based on a topological insulator, because any environmental doping will inevitably affect the surface state mobility, $\mu_S = e\ell_{\mathrm{tr}}/(\hbar k_F)$, in transport experiments. Even though the transport mean free path, ℓ_{tr}, might be significantly longer than ℓ, especially when backscattering is suppressed, our results indicate that mobilities will be reduced by the doping, implying that the full potential of TIs could only be realized in a controlled, preferably ultrahigh vacuum environment, or by an inert capping of the surface.

In conclusion, we have observed that the magnetic moment of an impurity does not play a dominant role in

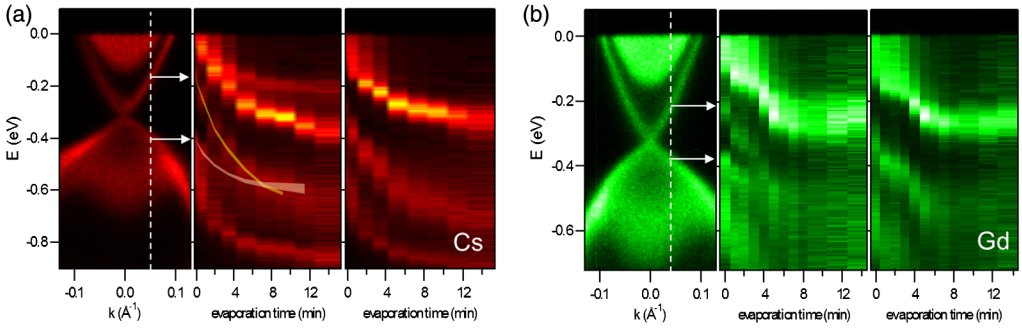

FIG. 4 (color online). (a) Development of the surface electronic structure with Cs doping. The middle panel shows the shift of the states at $k_x = 0.05$ Å^{-1}, while the right panel shows the Γ point in the surface BZ during Cs deposition. (b) Surface electronic structure upon Gd doping. The middle (right) panel represents the $k_x = 0.03$ Å^{-1}($k_x = 0$) point.

the scattering of the TSS. However, with the increasing doping, the state becomes warped, and the scattering eventually increases—irrespective of the impurity's magnetic moment. Therefore, the TSS does not remain protected indefinitely, even when doped with nonmagnetic impurities. Further, we have not seen any difference in the spectral region around the Dirac point between magnetic and nonmagnetic adsorbates, questioning previous claims that the observed spectral features indicate a magnetism-induced gap [17].

We acknowledge valuable discussions with G. Gu, P. D. Johnson, M. Khodas, R. Konik, and E. Vescovo. The work at BNL was supported by the US Department of Energy, Office of Basic Energy Sciences, under Contract No. DE-AC02-98CH10886. The work at MIT was supported by the US Department of Energy under Grant No. DE-FG02-07ER46134.

*valla@bnl.gov

[1] C. L. Kane and E. J. Mele, Phys. Rev. Lett. **95**, 146802 (2005).
[2] B. A. Bernevig, T. L. Hughes, and S. C. Zhang, Science **314**, 1757 (2006).
[3] M. Konig, S. Wiedmann, C. Brune, A. Roth, H. Buhmann, L. W. Molenkamp, X. L. Qi, and S. C. Zhang, Science **318**, 766 (2007).
[4] L. Fu, C. L. Kane, and E. J. Mele, Phys. Rev. Lett. **98**, 106803 (2007).
[5] H. J. Noh, H. Koh, S. J. Oh, J. H. Park, H. D. Kim, J. D. Rameau, T. Valla, T. E. Kidd, P. D. Johnson, and Y. Hu *et al.*, Europhys. Lett. **81**, 57006 (2008).
[6] D. Hsieh, D. Qian, L. Wray, Y. Xia, Y. S. Hor, R. J. Cava, and M. Z. Hasan, Nature (London) **452**, 970 (2008).
[7] H. J. Zhang, C. X. Liu, X. L. Qi, X. Dai, Z. Fang, and S. C. Zhang, Nature Phys. **5**, 438 (2009).
[8] D. Hsieh, Y. Xia, D. Qian, L. Wray, J. H. Dil, F. Meier, J. Osterwalder, L. Patthey, J. G. Checkelsky, and N. P. Ong *et al.*, Nature (London) **460**, 1101 (2009).
[9] Y. L. Chen, J. G. Analytis, J. H. Chu, Z. K. Liu, S. K. Mo, X. L. Qi, H. J. Zhang, D. H. Lu, X. Dai, and Z. Fang *et al.*, Science **325**, 178 (2009).
[10] Z.-H. Pan, E. Vescovo, A. V. Fedorov, D. Gardner, Y. S. Lee, S. Chu, G. D. Gu, and T. Valla, Phys. Rev. Lett. **106**, 257004 (2011).
[11] L. Fu, Phys. Rev. Lett. **103**, 266801 (2009).
[12] Q. Liu, C.-X. Liu, C. Xu, X.-L. Qi, and S.-C. Zhang, Phys. Rev. Lett. **102**, 156603 (2009).
[13] X. Zhou, C. Fang, W.-F. Tsai, and J. P. Hu, Phys. Rev. B **80**, 245317 (2009).
[14] H.-M. Guo and M. Franz, Phys. Rev. B **81**, 041102 (2010).
[15] R. R. Biswas and A. V. Balatsky, Phys. Rev. B **81**, 233405 (2010).
[16] Y. L. Chen, J. H. Chu, J. G. Analytis, Z. K. Liu, K. Igarashi, H. H. Kuo, X. L. Qi, S. K. Mo, R. G. Moore, and D. H. Lu *et al.*, Science **329**, 659 (2010).
[17] L. A. Wray, S. Y. Xu, Y. Xia, D. Hsieh, A. V. Fedorov, Y. S. Hor, R. J. Cava, A. Bansil, H. Lin, and M. Z. Hasan, Nature Phys. **7**, 32 (2010).
[18] P. Roushan, J. Seo, C. V. Parker, Y. S. Hor, D. Hsieh, D. Qian, A. Richardella, M. Z. Hasan, R. J. Cava, and A. Yazdani, Nature (London) **460**, 1106 (2009).
[19] T. Zhang, P. Cheng, X. Chen, J. F. Jia, X. C. Ma, K. He, L. L. Wang, H. J. Zhang, X. Dai, and Z. Fang *et al.*, Phys. Rev. Lett. **103**, 266803 (2009).
[20] T. Hanaguri, K. Igarashi, M. Kawamura, H. Takagi, and T. Sasagawa, Phys. Rev. B **82**, 081305 (2010).
[21] S. R. Park, W. S. Jung, C. Kim, D. J. Song, S. Kimura, K. D. Lee, and N. Hur, Phys. Rev. B **81**, 041405 (2010).
[22] H. M. Benia, C. Lin, K. Kern, and C. R. Ast, Phys. Rev. Lett. **107**, 177602 (2011).
[23] M. Bianchi, R. C. Hatch, J. Mi, B. B. Iversen, and P. Hofmann, Phys. Rev. Lett. **107**, 086802 (2011).
[24] H. Steinberg, D. R. Gardner, S. L. Young, and P. Jarillo-Herrero, Nano Lett. **10**, 5032 (2010).
[25] T. Valla, A. V. Fedorov, P. D. Johnson, B. O. Wells, S. L. Hulbert, Q. Li, G. D. Gu, and N. Koshizuka, Science **285**, 2110 (1999).
[26] W.-C. Lee, C. Wu, D. P. Arovas, and S.-C. Zhang, Phys. Rev. B **80**, 245439 (2009).
[27] K. Kuroda, M. Arita, K. Miyamoto, M. Ye, J. Jiang, A. Kimura, E. E. Krasovskii, E. V. Chulkov, H. Iwasawa, and T. Okuda *et al.*, Phys. Rev. Lett. **105**, 076802 (2010).